Söngen, Hagen; Rahe, Philipp; Neff, Julia L.; Bechstein, Ralf; Ritala, Juha; Foster, Adam; Kühnle, Angelika

The weight function for charges - A rigorous theoretical concept for Kelvin probe force microscopy

The weight function for charges—A rigorous theoretical concept for Kelvin probe force microscopy

Hagen Söngen, Philipp Rahe, Julia L. Neff, Ralf Bechstein, Juha Ritala, Adam S. Foster, and Angelika Kühnle

---

Articles you may be interested in

Potential Distribution in Functionalized Graphene Devices Probed by Kelvin Probe Force Microscopy
AIP Conf. Proc. **1399**, 819 (2011); 10.1063/1.3666628

Electrostatic depletion forces between planar surfaces
J. Chem. Phys. **128**, 164717 (2008); 10.1063/1.2908738

Driving forces behind ion-ion correlations
J. Chem. Phys. **125**, 236101 (2006); 10.1063/1.2403878

On the effect of image charges and ion-wall dispersion forces on electric double layer interactions
J. Chem. Phys. **125**, 154702 (2006); 10.1063/1.2357940

Kelvin probe force microscopy
Appl. Phys. Lett. **58**, 2921 (1991); 10.1063/1.105227

The weight function for charges—A rigorous theoretical concept for Kelvin probe force microscopy

Hagen Söngen,[1,2,a)] Philipp Rahe,[3] Julia L. Neff,[1] Ralf Bechstein,[1] Juha Ritala,[4] Adam S. Foster,[4] and Angelika Kühnle[1]

[1]*Institute of Physical Chemistry, Johannes Gutenberg University Mainz, Duesbergweg 10-14, 55099 Mainz, Germany*
[2]*Graduate School Materials Science in Mainz, Staudinger Weg 9, 55128 Mainz, Germany*
[3]*Department of Physics and Astronomy, The University of Nottingham, Nottingham NG7 2RD, United Kingdom*
[4]*COMP, Department of Applied Physics, Aalto University, PO Box 11100, FI-00076 Aalto, Finland*

A comprehensive discussion of the physical origins of Kelvin probe force microscopy (KPFM) signals for charged systems is given. We extend the existing descriptions by including the open-loop operation mode, which is relevant when performing KPFM in electrolyte solutions. We define the contribution of charges to the KPFM signal by a weight function, which depends on the electric potential and on the capacitance of the tip-sample system. We analyze the sign as well as the lateral decay of this weight function for different sample types, namely, conductive samples as well as dielectric samples with permittivities both larger and smaller than the permittivity of the surrounding medium. Depending on the surrounding medium the sign of the weight function can be positive or negative, which can lead to a contrast inversion for single charges. We furthermore demonstrate that the KPFM signal on thick dielectric samples can scale with the sample size—rendering quantitative statements regarding the charge density challenging. Thus, knowledge on the weight function for charges is crucial for qualitative as well as quantitative statements regarding charges beneath the tip. © *2016 AIP Publishing LLC.*
[http://dx.doi.org/10.1063/1.4939619]

I. INTRODUCTION

Kelvin probe force microscopy (KPFM) is a scanning force microscopy technique that has been adapted from the classical Kelvin probe[1] and is nowadays extensively used on a wide variety of samples and in various media.[2] The samples investigated so far can be classified into three types, namely, conducting, semi-conducting, and dielectric samples. While in most cases, the probe tip is scanned in vacuum or in air, KPFM instrumentation has recently been extended for operation in media like water,[3,4] hexane,[5] and other liquids.[6,7] KPFM signal generation has been investigated for a large number of systems,[2,7–9] including the contrast on different sample facets[10] and on metallic nanostructures[11,12] as well as at the atomic[13–17] and even submolecular[18,19] scale.

Recently, a very general electrostatic model from Kantorovich *et al.*[20] has been used in several case studies[21–23] to derive analytical expressions for the closed-loop amplitude modulation (AM)-KPFM and frequency modulation (FM-)KPFM signals measured for charged systems. In particular, this model separated the tip geometry from the sample charges as well as from the contact potential difference of the metallic contacts. However, closed-loop operation is incompatible with systems that must not be exposed to static electric fields[3,24–26] (e.g., electrolyte solutions).

Here, we will first extend this description to open-loop KPFM modes, where no DC bias voltage is applied. Based on Refs. 21–23, we second introduce a weight function that defines the contribution of each charge in the tip-sample system to the KPFM signals, both in the closed-loop and in the open-loop mode. Third, we systematically analyze this weight function for both conductive and thick dielectric samples as well as in media with different dielectric permittivities by considering a conductive sphere as a model for the probe tip. We will clarify under which circumstances a positive (negative) charge density underneath the probe tip shifts the KPFM signals to more positive (more negative) values, respectively. For the case of thick dielectric samples and a spherical tip, our analysis will reveal a possible dependence of the AM- and FM-KPFM signals on the size of the sample surface—consequently rendering quantitative statements of the charge density underneath the tip challenging.

II. THEORY AND METHOD

A. Electrostatic potential energy, tip-sample force, and force gradient

Kantorovich *et al.*[20] derived an expression for the electrostatic potential energy of a closed system of conductors and point charges, including an external battery to maintain constant potentials at the conductors. According to their treatment, the electrostatic potential energy U_{es} for an arrangement of two conductors with a potential difference V and N point charges $\{q_i\}$ at $\{\mathbf{r}_i\}$ in the space outside the conductors is given by[20,21]

a)soengen@uni-mainz.de

$$U_{\text{es}} = -\frac{1}{2}C_{\text{void}}V^2 + \sum_{i=1}^{N} q_i V \hat{\Phi}_{\text{void}}(\mathbf{r}_i)$$
$$+ \frac{1}{2}\sum_{i=1}^{N}\sum_{j=1}^{N} q_i q_j \Phi_{\text{ind}}(\mathbf{r}_i, \mathbf{r}_j) + U_{\text{C}}. \qquad (1)$$

In the above equation, C_{void} is the capacitance of the void tip-sample system (*without* point charges) and $\hat{\Phi}_{\text{void}}$ is the electrostatic potential of the void tip-sample system, normalized with respect to V using $\hat{\Phi}_{\text{void}} = \Phi_{\text{void}}/V$. The term Φ_{ind} $(\mathbf{r}_i, \mathbf{r}_j)$ is the potential at the position $\mathbf{r}_i$ due to the image charges induced in the conductors by a unit point charge at $\mathbf{r}_j$. The Coulomb energy U_{C} is constant, since we consider the positions $\{\mathbf{r}_i\}$ of the charges with respect to the sample fixed.[27] The last two terms of Eq. (1) do not depend on the potential difference V between the conductors.

In a typical KPFM setup, the two conductors represent the conductive probe and the conductive sample. In case of dielectric samples, the second conductor represents the conductive sample holder that acts as the back contact. In KPFM, a sinusoidal voltage with frequency ν_{es} and amplitude V_{es} as well as a DC bias voltage V_{bias} are applied between the conductive probe and the sample (or the sample holder). With a contact potential difference of V_{cpd} between the probe and the sample (or the sample holder), the potential difference between the two conductors is

$$V = V_{\text{es}}\cos(2\pi\nu_{\text{es}}t) + V_{\text{bias}} - V_{\text{cpd}}. \qquad (2)$$

Without loss of generality, the voltage is applied to the tip with the sample (or the sample holder) held at ground (Fig. 1).

The electrostatic force acting on the tip at a tip-sample distance z_{ts} can be obtained by differentiating the electrostatic potential energy with respect to the tip-sample distance, $F_{\text{es}} = -\partial U_{\text{es}}/\partial z_{\text{ts}}$. Substituting the expression for V [Eq. (2)] in Eq. (1) shows that the electrostatic force contains three spectral components,[8] namely, a DC component, the first harmonic at frequency ν_{es}, and the second harmonic at frequency $2\nu_{\text{es}}$. In the AM-KPFM mode, the spectral components of the probe deflection are detected. Here, the spectral component at the first and second harmonic of the electrostatic force is relevant.[21] Using the electrostatic description in Eq. (1) together with Eq. (2), the first and second

harmonic of the modulated electrostatic force (denoted as $F_{\text{es},1}$ and $F_{\text{es},2}$) at a fixed tip-sample distance z_{ts} is given by

$$F_{\text{es},1}(z_{\text{ts}}) = V_{\text{es}}\left(\frac{\partial C_{\text{void}}}{\partial z_{\text{ts}}}(V_{\text{bias}} - V_{\text{cpd}}) - \sum_{i=1}^{N} q_i \frac{\partial \hat{\Phi}_{\text{void}}(\mathbf{r}_i)}{\partial z_{\text{ts}}}\right),$$
$$(3)$$

$$F_{\text{es},2}(z_{\text{ts}}) = \frac{1}{4}\frac{\partial C_{\text{void}}}{\partial z_{\text{ts}}}V_{\text{es}}^2. \qquad (4)$$

In the FM-KPFM mode, the first and second harmonic of the eigen frequency shift is detected. In contrast to AM-KPFM, the first and second harmonic of the electrostatic force gradient $k_{\text{es}} = \partial F_{\text{es}}/\partial z_{\text{ts}}$ is relevant for the FM mode.[28,29] The first and second harmonic of the electrostatic force gradient (denoted as $k_{\text{es},1}$ and $k_{\text{es},2}$) at a fixed tip-sample distance z_{ts} is

$$k_{\text{es},1}(z_{\text{ts}}) = V_{\text{es}}\left(\frac{\partial^2 C_{\text{void}}}{\partial z_{\text{ts}}^2}(V_{\text{bias}} - V_{\text{cpd}}) - \sum_{i=1}^{N} q_i \frac{\partial^2 \hat{\Phi}_{\text{void}}(\mathbf{r}_i)}{\partial z_{\text{ts}}^2}\right),$$
$$(5)$$

$$k_{\text{es},2}(z_{\text{ts}}) = \frac{1}{4}\frac{\partial^2 C_{\text{void}}}{\partial z_{\text{ts}}^2}V_{\text{es}}^2. \qquad (6)$$

KPFM is typically performed in combination with conventional non-contact scanning force microscopy imaging where the probe tip is oscillated with an amplitude A along the tip-sample distance. Consequently, the main measurement signal is a convolution of the electrostatic force in AM-KPFM (force gradient in FM-KPFM) over different tip-sample distances during the oscillation[15,16,21,29] (see the Appendix for the full formulae).

In the following discussion, we will focus on qualitative aspects of the KPFM signals (i.e., the sign and the lateral decay of the weight function for charges). These qualitative statements can be made for arbitrary oscillation amplitudes, if the lateral decay and the sign of the quantity of interest are constant over the full oscillation cycle. As shown in detail later, this will be the case in most of the cases considered here.

B. The AM- and FM-KPFM signals

In closed-loop KPFM, a feedback loop is used to nullify the first harmonic component (of either the electrostatic force or the electrostatic force gradient) by adjusting the applied bias voltage. This adjusted bias voltage is hereafter referred to as the "KPFM signal" for the respective closed-loop case. Nullifying the first harmonic [Eqs. (3) and (5)] and solving for V_{bias} yield the same expressions that were deduced before[21–23] for the AM and FM-KPFM mode in the small amplitude approximation

$$V_{\text{AM}} = V_{\text{cpd}} + \sum_{i=1}^{N} q_i \frac{\partial \hat{\Phi}_{\text{void}}(\mathbf{r}_i)}{\partial z_{\text{ts}}} \bigg/ \frac{\partial C_{\text{void}}}{\partial z_{\text{ts}}}, \qquad (7)$$

$$V_{\text{FM}} = V_{\text{cpd}} + \sum_{i=1}^{N} q_i \frac{\partial^2 \hat{\Phi}_{\text{void}}(\mathbf{r}_i)}{\partial z_{\text{ts}}^2} \bigg/ \frac{\partial^2 C_{\text{void}}}{\partial z_{\text{ts}}^2}. \qquad (8)$$
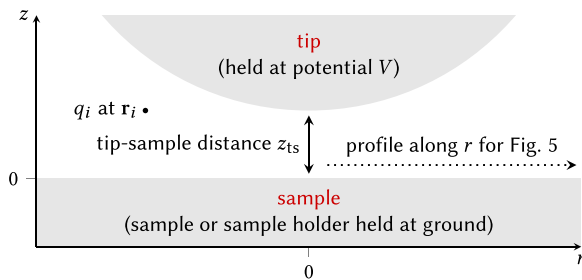

FIG. 1. Schematic view (not to scale) of the considered model for the probe tip and the flat sample. The spherical tip (which is not shown completely) is laterally centered at $r = 0$ and at a distance of z_{ts} above the sample surface, which is located at $z = 0$. A set of point charges $\{q_i\}$ at position $\{\mathbf{r}_i\}$ can be placed in the tip-sample system.

In open-loop KPFM both, the first and the second harmonic of either the electrostatic force or the electrostatic force gradient is recorded without applying a DC bias voltage ($V_{bias} = 0$). Dividing the respective first harmonic by the second harmonic leads to the expressions

$$V_{AM} = \frac{V_{es}}{4} \frac{F_{es,1}}{F_{es,2}}, \tag{9}$$

$$V_{FM} = \frac{V_{es}}{4} \frac{k_{es,1}}{k_{es,2}}. \tag{10}$$

Evaluating Eqs. (9) and (10) by using Eqs. (3)–(6) shows that open-loop KPFM allows for obtaining the same quantity as in the respective closed-loop KPFM mode. In the special case of no point charges present, this result has previously been obtained.[24,25,30] Here, we are able to show that this statement is also valid in the presence of arbitrary arrangements of charges in the tip-sample system.

The AM- and FM-KPFM signals are not only defined by the contact potential difference (between the tip and the sample or the sample holder in case of dielectric samples), but they also include a sum that contains the charges in the tip-sample system. Especially in case of thick dielectric samples, the contact potential difference depends on the material of the tip and the *sample holder*—providing no insights into properties of the sample itself. For these reasons, we focus on the contribution of the charges in the following discussion.

C. The weight function for charges

It is evident from Eqs. (7) and (8) that the first and second derivatives of $\hat{\Phi}_{void}$ and C_{void} with respect to the tip-sample distance z_{ts} are factors in the sum over the charges $\{q_i\}$. Thus, the ratio

$$w_{AM}(\mathbf{r}) \equiv \frac{\partial \hat{\Phi}_{void}(\mathbf{r})}{\partial z_{ts}} \bigg/ \frac{\partial C_{void}}{\partial z_{ts}} \tag{11}$$

can be considered as a weight function for charges in AM-KPFM, while the expression

$$w_{FM}(\mathbf{r}) \equiv \frac{\partial^2 \hat{\Phi}_{void}(\mathbf{r})}{\partial z_{ts}^2} \bigg/ \frac{\partial^2 C_{void}}{\partial z_{ts}^2} \tag{12}$$

defines the weight function for charges in FM-KPFM, both in the limit of small oscillation amplitudes (i.e., for a fixed tip-sample distance).[31] The weight functions (with the dimension of a voltage per charge) are evaluated at the individual positions of the charges $\{\mathbf{r}_i\}$ and, therefore, define the contribution of each charge in the tip-sample system to the KPFM signal. In the following, we will evaluate the sign and the lateral decay of the weight functions, which is mandatory to interpret KPFM signals with respect to the charge density underneath the tip.

D. General formulae

At this point, we are able to introduce a general formula for the KPFM signal V_{KPFM} of charged systems, in accordance with Ref. 21, including explicit formulae for arbitrary oscillation amplitudes:

$$V_{KPFM} = V_{cpd} + \sum_{i=1}^{N} q_i w(\mathbf{r}_i). \tag{13}$$

The weight function w is generally given as

$$w(\mathbf{r}) = \frac{\langle \hat{\Phi}_{void}(\mathbf{r}) \rangle}{\langle C_{void} \rangle}. \tag{14}$$

With the angle brackets we denote a functional given from the KPFM detection method and which is especially dependent on the oscillation amplitude. We state the functionals for the different KPFM modes in the Appendix. Here, we use the small amplitude approximation, where $\langle f \rangle = \partial f / \partial z_{ts}$ for AM-KPFM and $\langle f \rangle = \partial^2 f / \partial z_{ts}^2$ for FM-KPFM, respectively.

E. Model for tip and sample

To gain an understanding of the above terms $\hat{\Phi}_{void}$ and C_{void}, a specific model—applicable to scanning probe experiments—is considered here. To allow for a general discussion, we do not limit ourselves to a specific macroscopic tip model including the tip cone and the cantilever, but instead model the probe tip as a conductive sphere with radius R. This sphere model serves as a best-case scenario in terms of spatial resolution, which can be adjusted by varying its radius. For the discussion of the sign and the lateral decay of the weight function for charges, this model is expected to agree with a model including the tip cone and the cantilever. We confirmed that the conclusions regarding the lateral decay of the weight functions presented here are qualitatively reproduced by considering a more realistic probe geometry, namely, a spherical tip terminated by a cone on a disk-shaped cantilever[32] using the CapSol code by Sadeghi *et al.*[16] With this model, we also reproduced the sign of the weight function for charges directly beneath the tip in the relevant cases [(A), (B), and (C) for AM-KPFM as well as case (A) and (B) for FM-KPFM, the cases are introduced later in this section]. It is important to note, however, that we do not expect a quantitative agreement between calculations using the sphere model and more complex probe models.

Two sample types are considered: The sphere is placed either above a flat conductive or a thick (semi-infinite) flat dielectric sample. Expressions for the electrostatic potential and the capacitance of both systems have been derived in Refs. 16 and 33 using the method of image charges. The resulting equations were implemented in a Python script.[34]

The normalized electrostatic potential of the void tip-sample system $\hat{\Phi}_{void}$ and the capacitance C_{void} was calculated for different tip-sample distances in a range from $z_{ts} = R/40$ to $z_{ts} = 10R$. A typical tip curvature radius of $R = 20$ nm corresponds to a tip-sample distance range of 0.5 nm to 200 nm, which is a range that covers typical experiments for both small and large oscillation amplitudes. Second, we numerically calculated the first and second derivative of $\hat{\Phi}_{void}$ at each point in space with respect to the tip-sample distance z_{ts} using a second order central

difference approximation. Due to the axis-symmetry of the problem, cylindrical coordinates (r, z) are used. The derivatives of C_{void} were calculated accordingly.

The permittivity of the medium surrounding the tip is denoted as ε_{m}. When considering thick dielectric samples, the sample is described by its permittivity ε_{s}. In the following, we consider three different medium-sample systems:

- Case (A): a conductive sample.
  In this case, the normalized electrostatic potential is independent of the permittivity of the medium. Additionally, the capacitance of the tip-sample system scales linearly with the permittivity of the medium.[33] Thus, statements derived for this case hold true for a conductive sample with *any* kind of surrounding medium.
- Case (B): a thick dielectric sample in a medium with a 10 fold smaller permittivity than the sample ($\varepsilon_{\mathrm{s}}/\varepsilon_{\mathrm{m}} = 10$, e.g., a dielectric sample in vacuum).
- Case (C): a thick dielectric sample in a medium with a 10 fold larger permittivity than the sample ($\varepsilon_{\mathrm{s}}/\varepsilon_{\mathrm{m}} = 0.1$ representing a situation typically encountered in liquid media).

We exemplary plot the weight function for case (B) in Fig. 2. A dependence of both the magnitude and the sign of the weight function on the spatial variables (r, z) is clearly visible and will be analyzed in detail in the following discussion.

III. DISCUSSION

A. The capacitance

In this section, we discuss the capacitance C_{void} and its first and second derivative with respect to the tip-sample

distance as shown in Fig. 3. This discussion will be necessary to evaluate the sign of the weight function in Section III C.

In the case of conductive samples [case (A)], and in the case of thick dielectric samples in media with smaller permittivity than the sample [case (B)], the capacitance decreases upon increasing the tip-sample distance [Fig. 3(a)], resulting in a negative first derivative, $\partial C_{\mathrm{void}}/\partial z_{\mathrm{ts}} \leq 0$ [Fig. 3(b)]. This behavior is fundamentally different for dielectric samples in media with larger permittivity than the sample [case (C)]. Here, the capacitance *increases* with increasing tip-sample distance. Thus, the capacitance gradient, $\partial C_{\mathrm{void}}/\partial z_{\mathrm{ts}}$, is positive. This can intuitively be understood by considering the *averaged* permittivity of the volume surrounding the sphere. In case (B), the averaged permittivity increases upon decreasing the tip-sample distance (as $\varepsilon_{\mathrm{s}} > \varepsilon_{\mathrm{m}}$). In case (C), the average permittivity is decreased by decreasing the tip-sample distance (as $\varepsilon_{\mathrm{s}} < \varepsilon_{\mathrm{m}}$).

As shown in Fig. 3(a), the capacitance of the sphere above the sample approaches the capacitance of an isolated sphere in the respective medium ($\lim_{z_{\mathrm{ts}} \to \infty} C_{\mathrm{void}} = 4\pi\varepsilon_{\mathrm{m}}R$). Consequently, the first capacitance gradient approaches zero for large tip-sample distances in all considered cases [(A), (B), and (C)]. As a further consequence, the second capacitance gradient is positive in case of conductive samples [case (A)] and in case of thick dielectric samples in media with
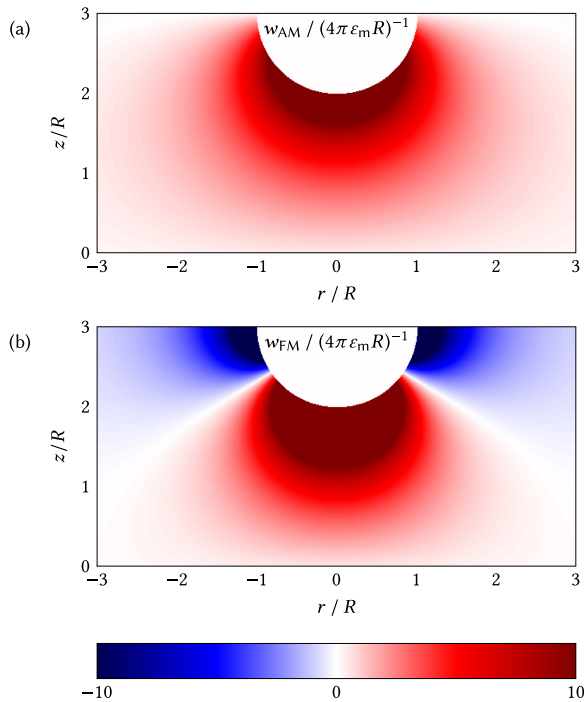
FIG. 2. Weight functions for case (B) with a tip-sample distance of $z_{\mathrm{ts}} = 2R$. The AM-KPFM weight function is shown in (a) and the FM-KPFM weight function in (b). The sample surface is located at $z = 0$. The color bar shown below applies for both plots.
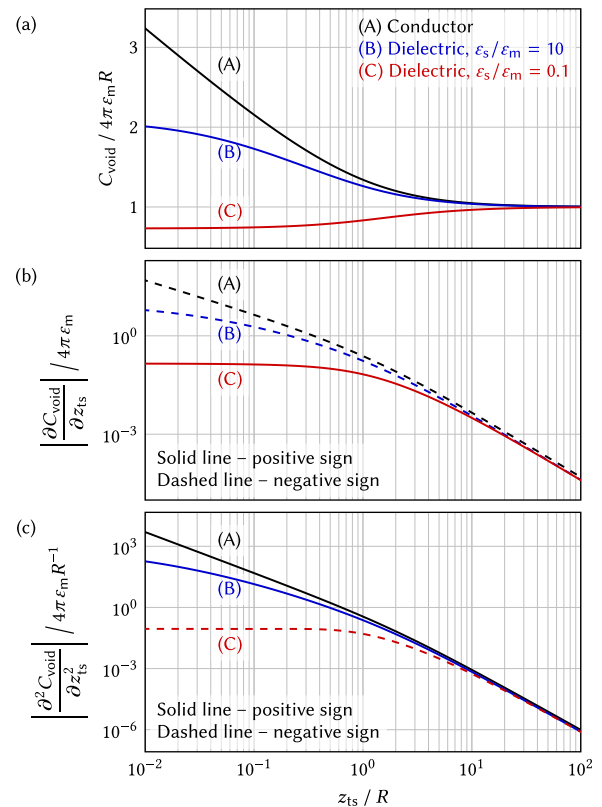
FIG. 3. (a) Capacitance C_{void} of the void tip-sample system as a function of the tip-sample distance z_{ts} for the three cases, namely, (A) conductive sample, (B) thick dielectric sample with $\varepsilon_{\mathrm{s}}/\varepsilon_{\mathrm{m}} = 10$, and (C) thick dielectric sample with $\varepsilon_{\mathrm{s}}/\varepsilon_{\mathrm{m}} = 0.1$. For large tip-sample distances, the capacitance of an isolated sphere in the respective medium is approached. The first and second derivatives of C_{void} with respect to the tip-sample distance z_{ts} (relevant for AM- and FM-KPFM, respectively) are shown in (b) and (c), respectively.

smaller permittivity than the sample [case (B)]. In contrast, the second capacitance gradient is negative for dielectric samples with a smaller permittivity than the medium [case (C)].

B. The normalized electrostatic potential

We now analyze the normalized electrostatic potential and its derivatives at the position of a single point charge in the tip-sample system. As a model system, we consider a point charge at a height of $z = 0.2$ nm above the sample. When choosing $R = 20$ nm, this height corresponds to $z = R/100$. Furthermore, we place the charge directly underneath the tip, i.e., at a lateral position of $r = 0$. It is not necessary to specify magnitude and sign of the point charge as the normalized electric potential is calculated for the *void* tip-sample system.

With a constant position of the charge (r, z), we present the normalized electrostatic potential and its derivatives for different tip-sample distances z_{ts} as shown in Fig. 4. As can be seen in Fig. 4(a), the electrostatic potential at the position of the considered charge decreases with increasing tip-sample distance. Consequently, the first derivative of the normalized electrostatic potential with respect to the tip-sample distance z_{ts} (relevant for AM-KPFM), as shown in Fig. 4(b), is negative in all considered cases.

The graphs of the second derivative $\partial^2 \hat{\Phi}_{void} / \partial z_{ts}^2$ as relevant for FM-KPFM are presented in Fig. 4(c). In the considered tip-sample distance range, the second derivative of the normalized electrostatic potential is positive for conductive

samples [case (A)] as well as for thick dielectric samples in a medium with a smaller permittivity than the sample [case (B)]. In contrast, the sign of the second derivative changes at a tip-sample distance of $z_{ts} \approx R/2$ from negative to positive when increasing z_{ts} in case (C). Consequently, for a correct qualitative interpretation of FM-KPFM signals in case (C), the tip-sample distance needs to be considered, since the FM-KPFM weight function can change the sign at different tip-sample distances when measuring on thick dielectric samples in media with larger permittivity than the sample.

C. The sign of the weight function for charges

Having analyzed the signs of the first and second derivatives of both the normalized electrostatic potential and the capacitance, we can now address the question whether a positive or negative charge density underneath the tip shifts the KPFM signal to more positive or more negative values. The sign of the relevant terms is summarized in Table I for a charge located directly underneath the tip (i.e., $r = 0$ and $0 < z < z_{ts}$).

On conductive samples [case (A)] and on thick dielectric samples in media with smaller permittivity than the sample [case (B)], indeed a positive (negative) charge density underneath the tip shifts the AM- and FM-KPFM signals to more positive (more negative) values, respectively. However, we find an exception to this generally assumed understanding for case (C) in the AM-KPFM mode. Here, in sharp contrast to what is observed for the other two cases, a *positive* charge density can result in a shift of the KPFM signal to *more negative* values and vice versa. This finding appears rather counterintuitive and clearly shows the challenges faced when interpreting KPFM signals.

In case (C), it is furthermore not possible to find a general statement for the FM-KPFM mode as the sign of w_{FM} changes with z_{ts} [Fig. 4(c)]. In case of finite oscillation amplitudes, this fact can cause an additional dependence on the oscillation amplitude due to the averaging, as described in the Appendix.

D. Lateral decay of the weight function for charges

So far, we considered the weight function for a single point charge at a height of $z = R/100$ situated underneath the tip at $r = 0$. On relevant samples, however, there are typically charges distributed across the whole sample surface. In
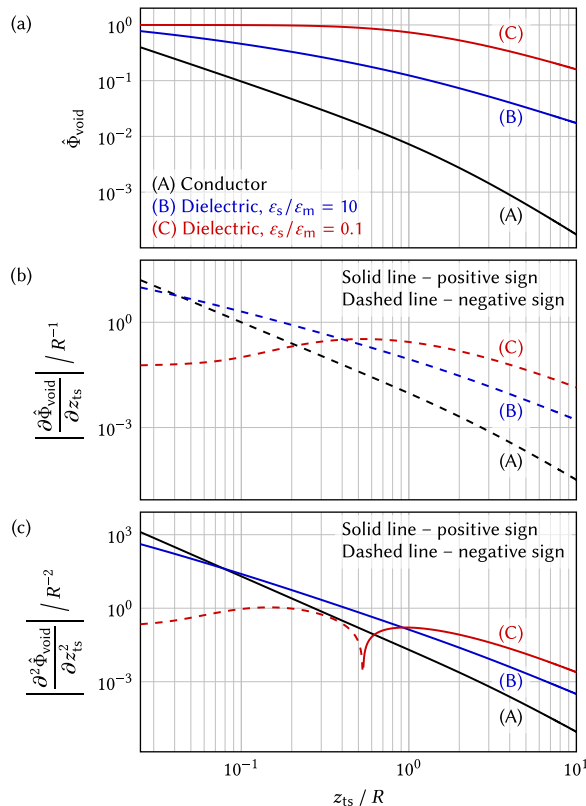

FIG. 4. (a) Normalized electrostatic potential at $r = 0$ and $z = R/100$ as a function of the tip-sample distance z_{ts} for the void tip-sample system. The first and second derivative with respect to the tip-sample distance z_{ts} (relevant for AM- and FM-KPFM) is shown in (b) and (c), respectively.

TABLE I. Sign of the relevant quantities when determining the charge density with KPFM for different types of medium-sample systems. The sign of the derivatives of the electrostatic potential was determined underneath the tip. The star symbol indicates that the sign of the respective quantity is dependent on the tip-sample distance; thus no general statement can be made here.

Medium-sample system		AM-KPFM			FM-KPFM		
	$\varepsilon_s/\varepsilon_m$	$\dfrac{\partial C_{void}}{\partial z_{ts}}$	$\dfrac{\partial \hat{\Phi}_{void}}{\partial z_{ts}}$	w_{AM}	$\dfrac{\partial^2 C_{void}}{\partial z_{ts}^2}$	$\dfrac{\partial^2 \hat{\Phi}_{void}}{\partial z_{ts}^2}$	w_{FM}
(A) Conductor		$-$	$-$	$+$	$+$	$+$	$+$
(B) Thick dielectric	10	$-$	$-$	$+$	$+$	$+$	$+$
(C) Thick dielectric	0.1	$+$	$-$	$-$	$-$	$\star$	$\star$

principle, each of these charges contributes to the KPFM signal according to the weight function for charges (w_{AM} and w_{FM}). Here, we address the significance of the contribution by charges far away from the probe tip.

We calculate the weight functions w_{AM} and w_{FM} according to Eqs. (11) and (12) at the same fixed height as before ($z = R/100$), but now as a function of the lateral distance r. We present the weight functions for the smallest considered tip-sample distance $z_{ts} = R/40$ in the left column of Fig. 5, while the right column shows the weight functions for the largest considered tip-sample distance of $10R$.

The AM-KPFM weight function w_{AM} is shown in Figs. 5(a) and 5(b), while the FM-KPFM weight function w_{FM} is shown in Figs. 5(c) and 5(d). The absolute values of the AM- and the FM-KPFM weight functions on conductive samples [case (A)] and on dielectrics samples with $\varepsilon_s > \varepsilon_m$ [case (B)] are at their maximum at $r = 0$; i.e., the charge density underneath the tip contributes most to the KPFM signals. For case (B), this can also readily be observed in Fig. 2. In contrast, on thick dielectric samples with $\varepsilon_s < \varepsilon_m$ [case (C) with $z_{ts} = R/40$], the maxima are not located directly underneath the tip, but at some distance $r \approx R$, both in AM- and in FM-KPFM [indicated by red arrows in Figs. 5(a) and 5(c)].

In case (B), the sign of the weight functions is independent of the lateral position r, while in cases (A) and (C), the AM-KPFM weight function w_{AM} approaches zero at some lateral distance $r \approx R$ and changes its sign for larger r [Figs. 5(a) and 5(b)]. For cases (A) and (C), a similar behavior can be observed for the FM-KPFM weight function, as is shown in Figs. 5(c) and 5(d). Consequently, depending on the lateral position r of a charge from the probe tip, the charge can contribute to the KPFM signal with an inverted sign.

As already discussed in Sec. III B, in case (C) the sign of w_{FM} underneath the tip changes when increasing the tip-sample distance from $R/40$ to $10R$. While this sign is positive

for a tip-sample distance of $R/40$ for the entire range of lateral distances r considered here [Fig. 5(c)], it is negative underneath the tip and changes to a positive sign at a lateral distance of $r \approx R$ for a tip-sample distance of $z_{ts} = 10R$ [Fig. 5(d)].

Next, we investigate the lateral decay of the weight function for charges by determining the slope of the weight functions for large r (by fitting the data shown in Fig. 5 with a power law). In the cases considered here, both the AM- and FM-KPFM weight functions (for $z = R/100$) decay with a fixed decay exponent α, according to the equations

$$\lim_{r \to \infty} w_{AM}(r) \propto r^{-\alpha}, \tag{15}$$

$$\lim_{r \to \infty} w_{FM}(r) \propto r^{-\alpha}. \tag{16}$$

This asymptotic behavior is the same in the considered tip-sample distance range, as indicated in Fig. 5. On conductive samples [case (A)], the decay exponent is $\alpha \approx 3$, both in AM- and in FM-KPFM. This is fundamentally different for thick dielectric samples [cases (B) and (C)], where we find for this setup $\alpha \approx 1$ again in both AM- and FM-KPFM.

Since the samples are typically significantly larger than R, the sample area containing charges that contribute to the KPFM signals is of relevance. Especially, we determine in the following whether this area is finite or whether it scales with the size of the sample surface. We discuss the two different cases ($\alpha \approx 1$ and $\alpha \approx 3$) in the limit of large r by considering a homogeneously charged layer with charge area density σ and radius r_σ on top of the (infinitely large) sample. The homogeneously charged layer is placed again at a height of $z = R/100$, with its center directly underneath the tip. We virtually increase the radius of the charged layer (while keeping the charge area density σ constant) to evaluate whether the KPFM signal converges. In case of conductive samples ($\alpha \approx 3$), the AM- and FM-KPFM signals converge with
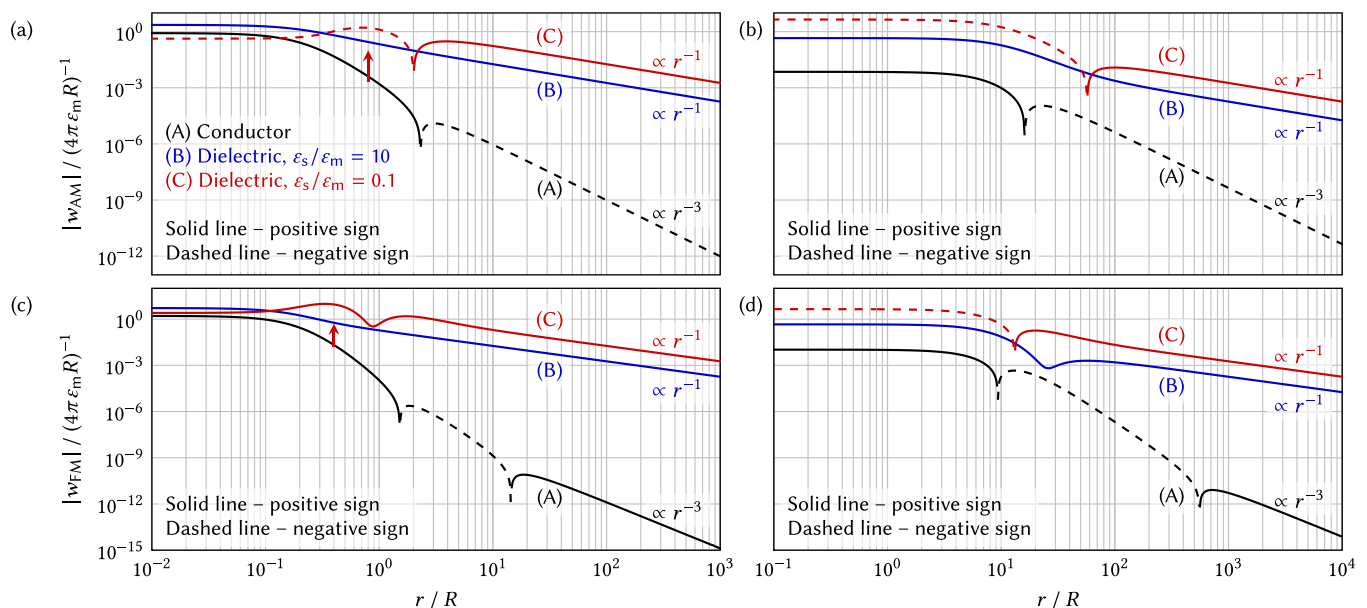

FIG. 5. Profile of the weight functions as a function of the lateral distance r for charges at a fixed height of $z = R/100$ above the sample. The AM-KPFM weight function is shown in (a) and (b), while the FM-KPFM weight function is shown in (c) and (d). In the left column [(a) and (c)], the tip-sample distance is $z_{ts} = R/40$ and in the right column [(b) and (d)] the tip-sample distance is $z_{ts} = 10R$.

respect to the considered radius of the layer, since the integral[35]

$$\lim_{r_\sigma \to \infty} \int_{r_0}^{r_\sigma} (2\pi r) r^{-\alpha} \sigma dr \propto \sigma \quad \text{for} \quad \alpha > 2 \qquad (17)$$

is finite and does not depend on r_σ (the factor $(2\pi r)$ arises from the integration in polar coordinates, r_0 is chosen sufficiently large so that the limit in Eqs. (15) and (16) remains valid). Thus, for conductive samples, the AM- and FM-KPFM signals at a given spot on the sample contain information on local charges underneath the tip, independent of the size of the sample surface—allowing a quantitative interpretation of the KPFM signal with respect to the charge density.

In case of thick dielectric samples [cases (B) and (C)], the weight function decays with $\alpha \approx 1$. We find that the AM- and FM-KPFM signals scale with r_σ, as can be seen from the integral

$$\int_{r_0}^{r_\sigma} (2\pi r) r^{-\alpha} \sigma dr \propto \sigma r_\sigma \quad \text{for} \quad \alpha \leq 2. \qquad (18)$$

Thus, if charges are equally distributed across the whole sample surface, the AM- and FM-KPFM signals can depend on the size of the sample surface since the integration over the weight function is diverging for the herein analysed setup. Furthermore, the difference between the KPFM signals above different spots of the sample is related to a *difference* in charge density underneath the tip—but a quantitative statement regarding the *absolute* value of the charge density beneath the tip requires not only knowledge of the weight function but furthermore an determination of the average charge density on the sample.

IV. CONCLUSION

In conclusion, we have extended the description of closed-loop KPFM signals to the open-loop KPFM mode for systems containing localized charges. Our analysis shows that open-loop KPFM allows for obtaining the same signal as in closed-loop KPFM, despite not applying a DC bias voltage in the open-loop mode, which is necessary for measurements in, e.g., electrolyte solutions. In both open- and closed-loop, as well as for AM and FM detection, the KPFM signals are a sum of the contact potential difference and a weighted addition over all charges in the tip-sample system. We introduced a weight function that describes the contribution of each charge to the KPFM signal. This weight function is defined by the detection mode and, especially, depends on the oscillation amplitude.

By using a conductive sphere as a model for the probe tip in KPFM, we investigated the sign of the weight function for charges. For conductive samples and for thick dielectric samples in media with smaller permittivity than the sample, a positive (negative) charge density underneath the tip shifts the AM- and FM-KPFM signals to more positive (more negative) values. However, when scanning on thick dielectric samples in a medium with larger permittivity than the sample, we find within our setup that the sign of the weight-function for charges underneath the tip is negative in case of AM-KPFM and that it changes sign for different tip-sample distances in the FM-KPFM mode. Consequently, a general statement regarding the sign of the weight function for FM-KPFM on a thick dielectric sample in a medium with a larger permittivity than the sample can only be made when the tip-sample distance and weight function are known. This illustrates that even the qualitative evaluation of the charge density beneath the tip with KPFM critically depends on the surrounding medium.

In an additional step, we compared the lateral decay of the weight function. On conductive samples, the weight function decays approximately with r^{-3}, both in AM- and FM-KPFM and in any surrounding medium. By considering a homogeneous surface charge on top of the sample, we concluded that in this case, the KPFM signal only contains contributions from charges in a finite area underneath the probe tip. Although the resolution will be limited by the tip size, a quantitative evaluation of the charge density in a finite area would be possible. However, we found for dielectric samples a lateral decay of the weight function with r^{-1} for all KPFM modes and independent of the permittivity of the surrounding medium. In this case, the absolute value of the KPFM signal can depend on the size of the sample surface and renders a quantitative evaluation of the absolute charge density values underneath the tip challenging.

We expect the above findings to be qualitatively reproduced by realistic probe geometries. Furthermore, our findings hold true regardless of the oscillation amplitude of the probe in the relevant cases [(A) and (B) for AM- and FM-KPFM as well as case (C) for AM-KPFM]. Therefore, our discussion of the weight function for charges is of general relevance for an improved understanding of KPFM. Our study demonstrates that a precise knowledge on the weight function for charges allows to discuss both quantitative and qualitative aspects of KPFM signals in all modes and in various medium-sample systems. Moreover, the knowledge of the weight function is of utmost importance for the interpretation of KPFM data with respect to the charge density beneath the tip, as even the sign for the KPFM signal of single charges can be inverted under certain conditions.

APPENDIX: THE AVERAGING FUNCTIONS DUE TO THE OSCILLATING PROBE TIP

As discussed in Sec. II A, the averaged electrostatic force (relevant for AM-KPFM) and the averaged electrostatic force gradient (relevant for FM-KPFM) are of

importance to account for the oscillation of the probe tip with an oscillation amplitude A and a minimum tip-sample distance $z_{ts,min}$ while performing the KPFM experiment. Both averaged quantities can be directly deduced from the electrostatic potential energy using the following functionals for arbitrary oscillation amplitudes, which are given according to the following Eqs. (A1) and (A2):[29,33]

$$\langle f \rangle_{AM} = \int_{-A}^{A} d\zeta \, u_{AM}(\zeta) \frac{\partial}{\partial z_{ts}} f(z_{ts,min} + A + \zeta),$$

$$\text{with} \quad u_{AM}(\zeta) = \frac{1}{\pi \sqrt{A^2 - \zeta^2}}, \tag{A1}$$

$$\langle f \rangle_{FM} = \int_{-A}^{A} d\zeta \, u_{FM}(\zeta) \frac{\partial^2}{\partial z_{ts}^2} f(z_{ts,min} + A + \zeta),$$

$$\text{with} \quad u_{FM}(\zeta) = \frac{2}{\pi A^2} \sqrt{A^2 - \zeta^2}. \tag{A2}$$

Thus, the averaged electrostatic force can be written as $\langle U_{es} \rangle_{AM}$ and the averaged electrostatic force gradient as $\langle U_{es} \rangle_{FM}$. Since the functions u_{AM} and u_{FM} are positive and independent of the tip-sample distance, the discussion concerning the lateral decay and the sign of the quantities described in Sec. II A is valid.

[1]M. Nonnenmacher, M. P. O'Boyle, and H. K. Wickramasinghe, Appl. Phys. Lett. **58**, 2921 (1991).

[2]W. Melitz, J. Shen, A. C. Kummel, and S. Lee, Surf. Sci. Rep. **66**, 1 (2011).

[3]N. Kobayashi, H. Asakawa, and T. Fukuma, Rev. Sci. Instrum. **81**, 123705 (2010).

[4]L. Collins, J. I. Kilpatrick, I. V. Vlassiouk, A. Tselev, S. A. L. Weber, S. Jesse, S. V. Kalinin, and B. J. Rodriguez, Appl. Phys. Lett. **104**, 133103 (2014).

[5]A. L. Domanski, E. Sengupta, K. Bley, M. B. Untch, S. A. L. Weber, K. Landfester, C. K. Weiss, H.-J. Butt, and R. Berger, Langmuir **28**, 13892 (2012).

[6]K. Umeda, K. Kobayashi, N. Oyabu, Y. Hirata, K. Matsushige, and H. Yamada, J. Appl. Phys. **113**, 154311 (2013).

[7]K. Umeda, K. Kobayashi, N. Oyabu, Y. Hirata, K. Matsushige, and H. Yamada, J. Appl. Phys. **116**, 134307 (2014).

[8]U. Zerweck, C. Loppacher, T. Otto, S. Grafström, and L. M. Eng, Phys. Rev. B **71**, 125424 (2005).

[9]M. Bieletzki, T. Hynninen, T. M. Soini, M. Pivetta, C. R. Henry, A. S. Foster, F. Esch, C. Barth, and U. Heiz, Phys. Chem. Chem. Phys. **12**, 3203 (2010).

[10]S. Sadewasser, T. Glatzel, M. Rusu, A. Jager-Waldau, and M. C. Lux-Steiner, Appl. Phys. Lett. **80**, 2979 (2002).

[11]C. Barth and C. R. Henry, Appl. Phys. Lett. **89**, 252119 (2006).

[12]C. Barth and C. R. Henry, J. Phys. Chem. C **113**, 247 (2009).

[13]L. Nony, A. S. Foster, F. Bocquet, and C. Loppacher, Phys. Rev. Lett. **103**, 036802 (2009).

[14]S. Sadewasser, P. Jelinek, C.-K. Fang, O. Custance, Y. Yamada, Y. Sugimoto, M. Abe, and S. Morita, Phys. Rev. Lett. **103**, 266103 (2009).

[15]S. Kawai, T. Glatzel, H.-J. Hug, and E. Meyer, Nanotechnology **21**, 245704 (2010).

[16]A. Sadeghi, A. Baratoff, S. A. Ghasemi, S. Goedecker, T. Glatzel, S. Kawai, and E. Meyer, Phys. Rev. B **86**, 075407 (2012).

[17]L. Gross, B. Schuler, F. Mohn, N. Moll, N. Pavliček, W. Steurer, I. Scivetti, K. Kotsis, M. Persson, and G. Meyer, Phys. Rev. B **90**, 155455 (2014).

[18]F. Mohn, L. Gross, N. Moll, and G. Meyer, Nat. Nanotechnol. **7**, 227 (2012).

[19]B. Schuler, S.-X. Liu, Y. Geng, S. Decurtins, G. Meyer, and L. Gross, Nano Lett. **14**, 3342 (2014).

[20]L. N. Kantorovich, A. I. Livshits, and M. Stoneham, J. Phys.: Condens. Matter **12**, 795 (2000).

[21]J. L. Neff and P. Rahe, Phys. Rev. B **91**, 085424 (2015).

[22]C. Barth, T. Hynninen, M. Bieletzki, C. R. Henry, A. S. Foster, F. Esch, and U. Heiz, New J. Phys. **12**, 093024 (2010).

[23]T. Hynninen, A. S. Foster, and C. Barth, e-J. Surf. Sci. Nanotechnol. **9**, 6 (2011).

[24]O. Takeuchi, Y. Ohrai, S. Yoshida, and H. Shigekawa, Jpn. J. Appl. Phys. **46**, 5626 (2007).

[25]L. Collins, J. I. Kilpatrick, S. A. L. Weber, A. Tselev, I. V. Vlassiouk, I. N. Ivanov, S. Jesse, S. V. Kalinin, and B. J. Rodriguez, Nanotechnology **24**, 475702 (2013).

[26]L. Kou, Z. Ma, Y. J. Li, Y. Naitoh, M. Komiyama, and Y. Sugawara, Nanotechnology **26**, 195701 (2015).

[27]It is important to note that the assumption of fixed charges may not be justified in liquids that contain mobile ions.

[28]T. R. Albrecht, P. Grütter, D. Horne, and D. Rugar, J. Appl. Phys. **69**, 668 (1991).

[29]F. J. Giessibl, Phys. Rev. B **56**, 16010 (1997).

[30]N. Kobayashi, H. Asakawa, and T. Fukuma, J. Appl. Phys. **110**, 044315 (2011).

[31]In case of finite oscillation amplitudes A, the weight functions are obtained by averaging the numerator and denominator in Eqs. (11) and (12) as described in the Appendix.

[32]The geometry of the full macroscopic probe is described by a tip radius of 20 nm, a cone height of 10 μm, a half opening angle of 25°, a cantilever radius of 40 μm and a cantilever thickness of 4 μm. The tip-sample distance was set to 0.5 nm. A sample thickness of 1 mm was considered in case of dielectric samples.

[33]A. Sadeghi, A. Baratoff, and S. Goedecker, Phys. Rev. B **88**, 035436 (2013).

[34]As shown in Refs. 16 and 33, the infinite series of image charges can be truncated and summed up analytically. We follow the therein described approach and checked all resulting quantities for convergence with respect to the truncation cut-off. See http://www.self-assembly.uni-mainz.de/software/kpfm_conducting_sphere.py for the Python source code for all calculations.

[35]The expression in Eq. (17) is derived from Eqs. (7) and (8) by writing the sum as an integral and separating the lateral distance ranges from $r \in [0, r_0]$ and $r \in [r_0, r_\sigma]$.